Mitochondrial survivin reduces oxidative phosphorylation in cancer cells by inhibiting mitophagy.

Running title: Survivin inhibits mitophagy.

Amelia R. Townley and Sally P. Wheatley

Abstract.

Survivin is a cancer-associated protein that is pivotal for cellular life and death: it is an essential mitotic protein and an inhibitor of apoptosis. In cancer cells, a small pool of survivin localises to the mitochondria, the function of which remains to be elucidated. Here, we report that mitochondrial survivin inhibits the selective form of autophagy, called "mitophagy", causing an accumulation of respiratory defective mitochondria. Mechanistically the data reveal that survivin prevents recruitment of the E3-ubiquitin ligase Parkin to mitochondria and their subsequent recognition by the autophagosome. The data also demonstrate that cells in which mitophagy has been blocked by survivin expression have an increased dependency on glycolysis. As these effects were found exclusively in cancer cells they suggest that the primary act of mitochondrial survivin is to steer cells towards the implementation of the Warburg transition by inhibiting mitochondrial turnover, which enables them to adapt and survive.

Introduction.

Survivin is a protein at the interface of cellular life and death, as it guides mitosis and inhibits apoptosis (Wheatley and Altieri, 2019). It is over-expressed in cancer and is associated with poor patient prognosis (Escuín and Rosell, 1999), reviewed in (Jaiswal *et al.*, 2015). Its abundance correlates directly to chemotherapy resistance highlighting it as a potential anti-cancer target (Morrison *et al.*, 2012). Survivin localises in several distinct pools (Fortugno *et al.*, 2002). During mitosis and as part of the chromosomal passenger complex, it directs chromosome congression and segregation, as well as cytokinesis. When present in interphase, its predominantly cytosolic localisation is key to its anti-apoptotic function (reviewed in (Wheatley and Altieri, 2019)). The focus of this paper is the mitochondrial pool of survivin, which is found only in cancer cells (Dohi *et al.*, 2004). What survivin does when resident in the mitochondria is a matter of ongoing debate (Hagenbuchner *et al.*, 2013; Rivadeneira *et al.*, 2015), although early evidence suggested that it may be a store of survivin with greater anti-apoptotic potential than the cytosolic pool "primed" in readiness to respond to pro-apoptotic signals (Dohi *et al.,* 2007).

Malignant transformation requires cellular changes that enable unrestricted proliferation and circumvention of programmes of cell death, such as apoptosis and autophagy. For decades the mitochondrion has been seen as a by-stander of malignant transformation, gaining inactivating mutations from various sources that switch cellular metabolism from oxidative phosphorylation (OxPhos) to glycolysis (Warburg, 1956). More recently it has begun to be appreciated that mitochondria actively participate in driving tumour progression and malignant transformation (Chatterjee *et al.*, 2011; Yadav and Chandra, 2013; van Gisbergen *et al.*, 2015)

Mitochondrial homeostasis, including their quality and length is maintained by the dynamic processes of fusion and fission, which are controlled by factors within the mitochondria and in the cytosol (Westermann, 2010; East and Campanella, 2016). In healthy cells, the balance between fusion and fission is tightly controlled to allow for the timely removal of non-functional mitochondria without affecting respiration (Nunnari *et al.*, 1997). In cancerous cells, this process is commonly deregulated resulting in the gradual accumulation of mitochondrial DNA (mtDNA) mutations that eventually trigger the loss of the respiratory apparatus (Balaban *et al.,* 2005; Porporato *et al.*, 2017), causing a reduction in OxPhos, and greater dependency on glycolysis, hence evoking the "Warburg Effect" (Merz and Westermann, 2009). In normal proliferating cells, fusion is important for the maintenance of healthy mitochondria as it can rescue damaged mitochondria by mixing their contents with healthy mitochondria (Westermann, 2010). Opposing fusion is fission, a process that generates mitochondrial fragments. In mitosis fission occurs to ensure that the organelle is correctly inherited (Twig *et al.,* 2008), but it is also necessary to maintain mitochondrial homeostasis as it precedes the removal of defective mitochondria by the selective form of autophagy, called "mitophagy" (Twig and Shirihai, 2011; Redmann *et al.*, 2014). Together, with mitochondrial biogenesis, mitophagy is a quality control mechanism that determines mitochondrial mass (Jornayvaz and Shulman, 2010).

Autophagy delivers defective organelles to autophagosomes, which fuse with lysosomes to degrade and recycle their constituents (Youle and Narendra, 2011). Organelles destined for recycling can be delivered to the autophagosome by two distinct pathways, either ubiquitin-dependent or ubiquitin-independent (Zaffagnini and Martens, 2016). The ubiquitin-dependent pathway requires ubiquitination of defunct organelles by E3-ubiquitin ligases and their subsequent recognition by ubiquitin binding proteins, which enables extension of the pre-autophagosomal (phagophore) membrane and their complete engulfment into the autophagosome (Shaid *et al.*, 2013). Mitochondrial recycling relies upon the action of PTEN-induced kinase 1 (PINK) and the E3-ubiquitin ligase Parkin (East and Campanella, 2016). Alterations to either of these processes result in the accumulation of defunct, metabolically inactive mitochondria. Reactive oxygen species (ROS), which are a principle cause of mitochondrial DNA (mtDNA) damage, are a by-product of OxPhos. If mitochondria harbouring mtDNA lesions are not removed in a timely manner they can promote tumourigenesis (Ott *et al.*, 2007). Cancer cells typically circumvent the damage by using glycolysis to generate ATP. Even though it is a less efficient means of ATP production, one of its major advantages is that it does not produce ROS and thus does not cause mtDNA mutations (Matthew G. Vander Heiden, 2009). Mitochondrial quality control is a relatively unexplored aspect of cancer, but given the accumulating evidence that alterations in mitophagy can bestow chemotherapy resistance (van Gisbergen *et al.*, 2015), understanding its contribution to the diseased state may reveal an Achilles' heel of cancer (Hagenbuchner *et al.*, 2013; Chourasia *et al.*, 2015; Vara-Perez *et al.*, 2019).

Here we test the hypothesis that survivin regulates mitochondrial homeostasis and respiratory dependence in cancer cells. We report that in cancer cells, survivin increases mitochondrial mass and reduces mtDNA quality by inhibiting mitophagy. We propose that as a consequence of accumulating a high load of respiratory inactive mitochondria, cancer cells with high expression of survivin reduces respiratory dependence on OxPhos forcing them to become more reliant on glycolysis for survival.

Results.

Survivin is found in the mitochondria of transformed cells.

It has previously been reported that a sub-population of survivin localises to the mitochondria in cancer cells. To verify that this was the case in the cells being examined here, we carried out subcellular fractionation to enrich for mitochondria in two cancerous lines: HeLa (cervical cancer) and U2OS (osteosarcoma), and in normal fibroblasts (MRC5), see Figure 1A. All lines were engineered to ectopically express survivin, C-terminally tagged with GFP or GFP alone (control). As indicated by enrichment of VDAC, and minimal contamination of tubulin (cytosolic marker) and histone H3 (nuclear marker), survivin-GFP was present in the mitochondria of HeLa and U2OS, but not MRC5 cells. These data corroborate previous work (Dohi *et al.*, 2004), and further demonstrate that this is also the case when survivin is present at high levels through ectopic expression.

Manipulating survivin expression alters mitochondrial mass.

To determine whether mitochondrial survivin can influence mitochondrial mass, we analysed whole cell extracts (WCE) of HeLa cells expressing GFP or survivin-GFP by immunoblotting (Figure 1B) and probed for anti-VDAC as a marker of mitochondrial mass. Semi-quantitative analysis of these blots (Figures 1C) was carried out by normalising the band intensity of the protein of interest against the anti-tubulin loading control and was presented as fold change of survivin-GFP compared with GFP. This analysis showed that VDAC levels increased significantly when survivin was expressed. In contrast to the results in HeLa cells, none of these alterations were observed in normal MRC5 fibroblasts expressing survivin-GFP (Figure 1D & E). To determine whether changes in expression of these proteins could be attributed to changes at the transcriptional level, quantitative PCR (qPCR) was performed on extracts from HeLa cells and fold change in expression between survivin-GFP and GFP controls plotted (Figure 1F). No change in VDAC mRNA was observed suggesting that the alterations occurred post-translation.

To further confirm that survivin expression increases mitochondrial mass, we quantified mitochondrial DNA (mtDNA) copy number. Genomic DNA was extracted from HeLa or MRC5 cells expressing either GFP or survivin-GFP, or after siRNA depletion. qPCR was used to determine the abundance of the mtDNA encoded tRNA(LEU) gene, which was then compared to the stably expressed nuclear reference genes ACTB (actin) and TUBB (tubulin). Fold change of RNA between cells expressing survivin-GFP and GFP was then calculated and presented on a Log_2 scale. Survivin overexpression increased mtDNA tRNA(LEU) gene expression in HeLa cells (Figure 1G), and decreased it in MRC5 cells (Figure 1H). Thus by an independent method, these data concur that mitomass is elevated by survivin expression in HeLa, but not MRC5 cells.

Having established that survivin overexpression increases mitomass, we next asked whether depleting it would have the opposite effect. To investigate this survivin-specific siRNA was performed (48h) on HeLa and MRC5 cells (Figure S1). WCEs were separated by SDS-PAGE, transferred to nitrocellulose and probed for VDAC as a

mitochondrial marker. Semi-quantitative analysis of blots was used to determine the fold change in siRNA treated versus untreated cells, normalised to tubulin. Survivin depletion caused a significant reduction in VDAC (Figure S1A and B). By contrast none of these effects were observed in MRC5 cells (Figure S1C and D). These data complement the overexpression data, and collectively prove that changes in survivin expression alter mitochondrial mass in some cancerous cells, but not in normal fibroblasts.

To determine whether the increase in mitomass was caused by elevated mitochondrial biogenesis, HeLa and MRC5 WCEs expressing GFP or survivin-GFP were run on an SDS-page gel, and immunoblotted for the biogenesis marker PGC1-α (Figure 1I and K). Semi-quantitative analysis showed that protein expression was decreased in HeLa cells (Figure 1J) and not altered in MRC5 cells (Figure 1L). Thus we conclude that the observed increase in mitomass is not due to increased mitochondrial biogenesis.

Finally, to determine whether mitochondrial survivin influences the expression of mitochondrial protein associated with fission or fusion, we analysed whole cell extracts (WCE) of HeLa cells expressing GFP or survivin-GFP by immunoblotting (Figure S1E) and probed for fission proteins DRP1 and FIS1, as well as the fusion proteins, OPA1 and MFN1/2, using tubulin as a loading control and VDAC as a marker of mitochondrial mass. Semi-quantitative analysis was calculated as described previously and presented as fold change of survivin-GFP compared with GFP (Figure S1F). This analysis demonstrated a statistical increase in DRP1, OPA1 and MFN2 expression, which was removed when the data were normalised to VDAC to account for mitochondrial mass alterations (Figure S1G). A statistical decrease in FIS1 expression was still observed when normalised to VDAC, demonstrating a potential mitomass-independent alteration to FIS1 levels. None of these changes were observed in normal MRC5 fibroblasts expressing survivin-GFP (Figure S1H/I). Collectively, these data demonstrate that the observed increase in mitomass observed in HeLa cells cannot be attributed to changes in the expression of fission and fusion factors associated with mitochondrial dynamics. Survivin does not alter mitochondrial morphology or polarisation in HeLa cells.

Next, to clarify whether alterations to mitomass are caused by changes to mitochondrial dynamics, we used a combination of fluorescent mitochondrial stains and live imaging to observe the total mitochondrial network in HeLa cells transiently overexpressing GFP/RFP or survivin-GFP/survivin-RFP and labelled with MitoTracker Red (Figure 1M, colour in S2) to visualise the mitochondrial network and found no gross abnormalities in terms of their overall appearance, categorised as normal or fragmented (Figures 1N). However, consistent with the immunoblotting and qPCR data, when MitoTracker Green was used to measure total pixel area in RFP/Survivin-RFP expressing cells it was apparent that mitochondrial area was significantly higher in survivin expressing cells (Figure 1O). Note that GFP and RFP labels used interchangeably, and selected due to availability of relevant mitotracker dyes. We then monitored alterations to mitochondrial membrane potential using MitoTracker Far Red; a fluorescent stain that highlights polarised mitochondria specifically. The average signal intensity was quantified and normalised to MitoTracker Green to

account for mitochondrial mass (MTFR:MTG). As shown in Figure 1P, in HeLa cells mitochondrial polarisation was not affected by survivin expression. Thus we conclude that survivin expression causes an increase in mitomass as judged by the area that they cover but that the mitochondria held their membrane potential.

Forced mitochondrial localisation of survivin in normal fibroblasts increases mitomass.

To assess whether the effects to mitomass were due specifically to the mitochondrial localisation of survivin, we utilised a survivin-GFP construct tagged with a *bona fide* mitochondrial targeting sequence (MTS) from cytochrome c oxidase subunit VIIIA, and forced it to be mitochondrial in normal fibroblasts (Figure 2A). Immunoblots of WCEs from MRC5 cells expressing GFP, SVN-GFP or MTS-SVN-GFP were probed for anti-VDAC to assess mitochondrial mass, and PGC1-α to assess alterations to mitochondrial biogenesis (Figure 2B). Semi-quantitative analysis of protein expression normalised to tubulin showed that forced mitochondrial localisation of survivin in MRC5 cells significantly increased VDAC expression (Figure 2C), without altering expression of the mitochondrial biogenesis protein PGC1-α (Figure 2D). This suggests that mitochondrial localisation of survivin can account for an increase in mitochondrial mass.

Survivin does not inhibit mitophagic steps preceding mitochondrial translocation of Parkin.

As the experiments described thus far suggested that survivin increases mitochondrial mass independently from mitochondrial biogenesis or dynamics, we next asked whether changes to the selective autophagic process of "mitophagy" could be responsible. Defective regions of the mitochondrial network with depolarised membranes due to their inactivity are selected for degradation by the process of mitochondrial fission. Mitophagy is then triggered by the accumulation of full-length PINK1 spanning the OMM, which phosphorylates both outer-membrane protein targets as well as the E3-ubiquitin ligase Parkin, causing its translocation from the cytosol to the OMM.

To discover where survivin operates in the mitophagic pathway, first HeLa cells expressing GFP/survivin-GFP or RFP/survivin-RFP were treated with FCCP (10 μM) to depolarise the mitochondria and stimulate mitophagy. To ensure that the effects were mitophagy specific and that there was no influence from apoptotic activity, the experiment was carried out over 3 hours, (see (Dispersyn *et al.*, 1999). Cells were then stained with MitoTracker Red to visualise the mitochondrial network, and MitoTracker Green/MitoTracker Far Red to determine membrane polarisation respectively. As shown in Figure 3A and B, FCCP caused mitochondrial fission similarly in both cell lines, demonstrating that survivin cannot stop chemically triggered mitochondrial fragmentation. Under these conditions, survivin expression also did not prevent OMM depolarisation (Figure 3C).

Next, to determine whether survivin alters PINK1 stabilisation, HeLa, U2OS or MRC5 cells were treated with FCCP (10 μM) and CQ (100 μM) for 6, 12 or 24 h, WCE were prepared and immunoblots probed for PINK1 to determine its stability post

mitophagy stimulation (Figure 3D, F and H). Semi-quantification revealed no alterations to PINK1 stabilisation over the time course in any of the cell lines (Figure 3E, G and I). Finally, to determine if survivin alters the interaction of PINK1 and its target E3-ubiquitin ligase Parkin, we performed a pulldown with recombinantly expressed GST-Parkin in the presence of a HeLa WCE expressing GFP or survivin-GFP (Figure 3J). Immunoblotting of the GST-pulldown assay shows survivin does not alter the interaction of PINK1 and GST-Parkin.

Survivin prevents Parkin recruitment to the mitochondria.

We then asked whether survivin alters the recruitment of Parkin to the mitochondria post mitophagy stimulation. To address this, HeLa and MRC5 cells were transiently transfected with the mitophagy-specific E3-ligase, Parkin, N-terminally tagged with mCherry (a gift from Prof. S. Martin, Dublin), and FCCP-treated, then labelled with mitotracker far red and analysed by fluorescence imaging. Here a marked difference was seen: mCherry-Parkin was recruited to the mitochondria of GFP-HeLa cells after FCCP treatment, but it was retained in the cytoplasm in survivin-GFP cells (Figure 4A), and this trend was confirmed by phenotype counting and quantification (Figure 4B). Conversely, the mitochondrial recruitment of mCherry-Parkin was unaffected in MRC5 cells expressing survivin-GFP (Figure S3, quantification shown in Figure 4C). From this we conclude that after mitochondrial fragmentation and depolarisation, survivin prevents Parkin recruitment from the cytosol to the mitochondria, which blocks mitophagy in cancer cells.

Survivin decreases mitochondrial co-localisation with lysosomes after mitophagy stimulation.

To further confirm how survivin affects mitophagy, HeLa cells expressing RFP or SVN-RFP were treated with FCCP as previously described, and stained with LysoTracker Blue to observe autophagosomes, and MitoTracker Green to observe mitochondria (Figure 5A, see S4 for full gallery). Co-localisation analysis was then carried out to assess the proportion of the mitochondrial network that co-localised with lysosomes. This demonstrated that post FCCP treatment, significantly more mitochondria and lysosomes co-localised in RFP-expressing cells than in SVN-RFP cells, as shown by pixel intensity line plots (Figure 5B arrows, and 5C) and whole pixel co-localisation analysis of images (Figure 5D).

Survivin mimics the effect of Bcl-2 upon mitophagy.

Having established that mitochondrial survivin increases mitomass by inhibiting mitophagy, we next asked whether survivin cooperates with an apoptotic collaborator, Bcl-2, in this process. To address this, HeLa cells expressing GFP or survivin-GFP were treated with the Bcl-2 inhibitor Navitoclax (1µM) and 10 µM FCCP to stimulate mitophagy post transfection with mCherry-Parkin. Here, mCherry-Parkin translocation to the mitochondrion was increased after FCCP treatment with Navitoclax in cells expressing survivin-GFP, but not in GFP expressing cells (Figure S5A) quantified in (Figure S5B). A UV dose response curve was simultaneously performed to prove that Navitoclax (1µM) was sufficient to inhibit Bcl-2 activity

(Figure S5C). From these data we conclude that the effect of survivin on mitophagy may be enhanced via collaboration with Bcl-2.

Survivin compromises mtDNA integrity.

As the role of mitophagy is to eliminate defective mitochondria, we next examined the quality of accumulated mtDNA using a PCR-based lesion frequency assay. Briefly, genomic DNA was prepared from cells as described for Figure 1G and H and PCR reactions carried out to produce either a 'long read' (9kb) or a 'short read' (150 bp) product. In this lesion assay if mtDNA is intact both products will be generated, however, if the DNA polymerase encounters lesions, it will stall and less 9kb product will form. The 150 bp product is used as a loading control. As shown in Figure 6A, fewer 9kb product was generated in HeLa cells expressing survivin, compared to the GFP control, a difference that, when normalised to the 150 bp was highly significant (Figure 6B). Conversely the 9kb was not only retained but actually increased upon survivin depletion from HeLa cells (Figures 6C and D). In contrast, in MRC5 cells depleting survivin had no effect (Figure 6E and F). Taken together these data suggest that survivin reduces the quality of mtDNA specifically in cancer cells.

Survivin expression phenocopies chloroquine treatment and reduces oxidative phosphorylation in cancer cells.

Based on the observations thus far we hypothesised that survivin inhibits the removal of defective mitochondria by mitophagy, reducing overall mitochondrial quality. To test this, cells over-expressing GFP or survivin-GFP were exposed to the autophagy inhibitor chloroquine (CQ) for 16h, the mitochondria isolated and a resazurin assay performed to assess their respiration. As shown in Figures 7A-D, CQ treatment (50 and 150 μM) reduced metabolism of mitochondria isolated from GFP-expressing HeLa or U2OS cells, which is consistent with a block on the removal of defunct mitochondria. By contrast, mitochondria isolated from survivin-GFP cells, which showed reduced respiration in the absence of CQ. After CQ exposure, this survivin-induced suppression of metabolism did not reduce further, but actually showed a slight elevation, for reasons that remain unclear. Consistent with the lack of survivin in the mitochondria of normal cells, there was no significant difference in the respiratory profiles of mitochondria isolated from MRC5 GFP or survivin-GFP cells, which responded similarly t to CQ (Figure 7E and F). Taken together these data suggest that survivin expression in cancer cells represses mitochondrial metabolism and phenocopies CQ treatment.

Having shown that mitochondrial quality is impaired by survivin up-regulation, we next asked directly whether survivin expression affected mitochondrial oxidative phosphorylation. To address this a resazurin assay was carried out every 30 minutes over 4h on mitochondria isolated from HeLa, U2OS or MRC5 cells (Figure 8). Both HeLa and U2OS cells expressing survivin-GFP showed a significant decrease in resorufin fluorescence compared to GFP expressing cells (Figure 8A & C). To ensure the observed alterations were most likely due to changes in OxPhos rather than the mitochondrial TCA cycle, we also determined the response of each line to the complex V inhibitor, oligomycin (Figures 8B, D and F). Mitochondria isolated from

both HeLa and U2OS cells expressing GFP were more sensitive to oligomycin than those from survivin-GFP cells (Figure 8B & D), suggesting that survivin significantly reduced OxPhos in cancer cells. In contrast, no significant difference was seen in the ability of MRC5-derived mitochondria to metabolise resazurin (Figure 8E and S6). Furthermore, forced mitochondrial localisation of survivin in MRC5 cells using MTS-SVN-GFP, was able to reduce mitochondrial metabolism in the same manner as in SVN-GFP expressing HeLa and U2OS cells (Figure 8F). From these data we conclude that survivin can inhibit reduction reactions when present within mitochondria.

Survivin expression increases glucose consumption and lactate production.

As survivin overexpression was found to reduce OxPhos, our final question was whether cancer cells compensated for this reduction by increasing glycolytic respiration. To test this we used luciferase-based assays to measure glucose consumption and lactate production. Survivin-GFP HeLa cells had a significantly lower glucose concentration (Figure 8G) and higher rate of lactate production (Figure 8H) compared to GFP expressing cells 2h post-seeding. Moreover, the rates at which glucose was consumed and lactate concentration rose was significantly higher than those observed in GFP cells. As both cell lines grew at the same rate (Figure 8I), we conclude that the differences observed were due primarily to metabolic adjustments and not differences in proliferation.

Discussion.

Survivin is an essential protein that is deregulated in cancer, becoming present throughout the cell cycle, rather than being confined to G2 and M-phases (Barrett *et al.*, 2009). In transformed cells in interphase it is predominantly cytoplasmic, shuttling between the cytoplasm and nucleus in a CRM1/exportin-dependent manner (Colnaghi *et al.*, 2006; Engelsma *et al.*, 2007; Stauber *et al.*, 2007). Cytoplasmic survivin inhibits apoptosis, and it has been suggested that prior residence in the mitochondria can enhance this activity (Dohi *et al.*, 2007). Consistent with previous studies (Dohi *et al.*, 2004; Dohi *et al.*, 2007; Hagenbuchner *et al.*, 2013, 2016; Rivadeneira *et al.*, 2015), we have found that survivin only accesses the mitochondria of transformed cells. Although survivin is essential, presumably its mitochondrial residence is not, and constitutes a gain of function over its normal roles.

In this study we tested the hypothesis that survivin interferes with mitochondrial homeostasis and alters respiratory dependence in cancer cells. Mitochondria are dynamic organelles that regulate cellular metabolism and survival. The opposing pathways of mitochondrial biogenesis and autophagic degradation control their quantity and quality. Combined with fusion and fission, these mechanisms govern mitochondrial activity (Palikaras *et al.*, 2015), and alterations to any one of these processes have been linked to ageing and disease (Redmann *et al.*, 2014). In cancer cells these processes are often deregulated, consequently mitochondrial health is compromised: mtDNA harbouring mutations accumulate, respiratory efficiency declines, and ultimately cells switch from OxPhos to glycolytic dependence (Merz and Westermann, 2009) (Sumpter *et al.*, 2016). OxPhos itself plays a major role in mtDNA damage as it produces ROS that continuously bombard the mtDNA causing lesions (Ray *et al.*, 2012; Sabharwal and Schumacker, 2014). Healthy cells respond to this damage by removing the affected sections of mitochondria using a selective form of autophagy called “mitophagy” (see Figure S8).

Mitophagy commences with mitochondrial fission, which produces asymmetrical daughter mitochondria, one with an increased membrane potential that can fuse with healthy mitochondria (Twig, Elorza, *et al.*, 2008), and one with a depolarised membrane that is targeted for mitophagy (Elmore *et al.*, 2001; Nicholls, 2004). Depolarisation of the OMM of defunct mitochondria stabilises the serine/threonine kinase PINK1, which phosphorylates the E3-ligase Parkin at Ser65, and activates it. Parkin then accumulates at the OMM (Vives-Bauza *et al.*, 2010; Youle and Narendra, 2011) where it mediates ubiquitination of VDAC1 (Kazlauskaite *et al.*, 2014). In turn VDAC-ubiquitination stimulates translocation of the autophagic adaptor protein, p62 to the mitochondria, which signals their engulfment by pre-autophagosomes via interaction with LC3 (Lee *et al.*, 2010; East and Campanella, 2016).

As indicated by increased expression of VDAC, mtDNA copy number and MitoTracker Green pixel area, ectopic expression of survivin caused an increase in total mitochondrial mass. We also noted that VDAC was being affected post-translation, while FIS1 levels, which decreased when survivin levels were elevated, were affected by transcriptional repression. We have also found that survivin does not increase

mitochondrial biogenesis, nor does it alter mitochondrial dynamics, which contrasts with findings in neuroblastoma (Hagenbuchner *et al.*, 2013). Subsequent data suggest that in the cancer cells observed here, survivin increases mitochondrial mass by preventing mitochondrial translocation of Parkin, which arrests the mitophagic process by preventing lysosomes from colocalising with, and degrading defective mitochondria (Figure S7). Moreover, through the use of a *bona fide* mitochondrial-targeting signal from cytochrome c oxidase subunit VIIIA (MTS-SVN-GFP) we were able to force non-cancerous MRC5 cells to behave like the cancerous cells, and thus to demonstrate that the changes that we have reported can be attributed specifically to the presence of survivin in the mitochondria.

In addition to the increase in mitomass, we found that cancerous cells expressing survivin had poor quality mtDNA, and that survivin suppressed OxPhos and increased respiratory dependency on glycolysis in these cells. Additionally, through the use of MTS-SVN-GFP we were able to reduce mitochondrial metabolism in non-cancerous MRC5 cells similarly to wild type survivin in HeLa cells. It is well documented that when mitophagy is inhibited, mitochondria with mtDNA lesions accumulate within the cell. This can directly impact the activity of mtDNA encoded proteins, notably members of the electron transport chain (Sumpter *et al.*, 2016) which directly impacts mitochondrial metabolism. Mitophagy can be artificially blocked using general autophagy inhibitors, such as CQ, which has been shown to reduce mitochondrial metabolism in the described manner (Redmann *et al.*, 2017). Here, we saw no further reduction in the respiration of mitochondria isolated from survivin-GFP expressing cancer cells after treatment with CQ, therefore allowing us to conclude that survivin modifies mitochondrial metabolism specifically due to alterations to mitophagy. Survivin inhibits mitophagy, causing an accumulation of respiratory defective organelles which in turn reduces OxPhos (Redmann *et al.*, 2017). Moreover, as OxPhos was altered to the same degree by CQ treatment in MRC5 cells irrespective of survivin expression, we conclude that this change is due to the mitochondrial pool of survivin.

When determining where survivin acts in the mitophagic pathway, we found that neither mitochondrial fragmentation, OMM depolarisation, PINK1 stabilisation nor its interaction with the E3 ubiquitin ligase Parkin was affected. Instead survivin prevents the recruitment of Parkin to the mitochondria. It has previously been reported that survivin inhibits the activities of PINK/Parkin, and that this response causes survivin degradation (Hagenbuchner *et al.*, 2016). While our study also links survivin and Parkin, we offer a slightly alternative interpretation: rather than causing its own demise, survivin inhibits mitophagy by preventing Parkin from translocating to the mitochondria, and the resulting accumulation of mitochondria with damaged mtDNA ultimately forces the cell to switch from oxidative phosphorylation to glycolysis. As we have previously shown that survivin can inhibit autophagic flux (Humphry and Wheatley, 2018), we suggest that survivin can interfere with mitophagy both by inhibiting Parkin recruitment to the OMM, and later, preventing flux (Figure S7). Although a less efficient means of respiration, glycolysis produces less ROS, and thus, in addition to the initial survival response, this switch can provide cancer cells with a further survival advantage.

Our findings with survivin mirror these described by (Hollville *et al.*, 2014), in a series of experiments examining the role of the apoptosis inhibitor BCL-2. Accordingly, treatment with the BCL-2 inhibitor Navitoclax partially recovered the translocation of Parkin to the mitochondria, suggesting survivin acts in this process through a collaboration with BCL-2.

Finally, as none of these changes occurred in normal fibroblasts in which survivin is not mitochondrial, and in fact forcing survivin into the mitochondria of these cells increases mitomass and decreases metabolism, we conclude that the effects are exclusive to cancer cells and can be attributed solely to the mitochondrial pool of survivin. The targeting of mitochondrial survivin and the metabolic alterations it provides cancerous cells, could therefore offer a distinct opportunity to develop novel therapeutic treatments with reduced off target effects in non-cancerous cell lines.

Materials and Methods.

All reagents were obtained from Sigma unless specified.

Human Cell Culture.

Human epithelial carcinoma cells (HeLa, ATCC), Osteosarcoma (U2OS), and normal lung fibroblasts (MRC5 :Medical Research Council Strain 5, Genome and Stabiility Centre, Sussex), were cultured in 5% CO_2 at 37°C with humidity in Dulbecco's Modified Eagle's Medium (DMEM, Gibco, Invitrogen) supplemented with 4 mM L-glutamine, 10% Fetal Calf Serum (FCS, Thermo Scientific), 244 µM penicillin and 172 µM streptomycin. Derivative lines expressing GFP or survivin-GFP were maintained under the selection pressure of 1 mM G418 (Fisher). Experiments were carried out on cells within 30 passages.

DNA and siRNA Transfections.

Cells were seeded into a relevant dish or imaging chamber in antibiotic free media, incubated for 12 h before transfection and left for approximately 48 h before use. DNA transfections were performed using Torpedo Transfection reagent (Ibidi) and 0.3 µg of relevant DNA construct (see Table S1), as per the manufacturer's guidelines. siRNA transfections were performed using HiPerfect transfection reagent (Qiagen) and 75 ng of relevant siRNA, as per the manufacturer's instruction.

Cell counting assay.

Cells were seeded at a density of 200 cells per 10 cm petri dish, and the number of cells in individual colonies after 8, 24, 48 and 72 h.

Immunoblotting.

Protein samples were separated according to standard procedures using 12% acrylamide SDS-PAGE gels, in running buffer (25 mM Tris, 192 mM glycine, 0.1% (w/v) SDS) and transfer onto a 0.22 µM nitrocellulose membrane (BIOTRACE, PALL life sciences) using transfer buffer (24 mM Tris, 195 mM glycine, 0.1% SDS, 10% methanol). Post-transfer membranes were blocked with 5% non-fat milk (Marvel, in PBS +0.1% Tween 20 (PBST)) then incubated with appropriate primary antibody overnight at 4°C, washed three times with PBST then incubated in the appropriate horseradish peroxidase conjugated secondary antibody (see 3.5) in 5% non-fat milk. EZ-ECL chemilluminescence detection reagent was then added (Geneflow) and membrane exposed to detection film (Roche).

Immunoblots were quantified using Fiji software. Band intensity peaks were measured and combined into sample groups for each condition. Within each pool, intensity values for each protein were expressed as a percentage of the loading control average and then as a percentage of the control protein average. The final expression value was presented as a decimal and transformed as a function of a base 2 logarithm (log_2).

Mitochondrial DNA lesion assay.

2 x 10^6 cells were washed with PBS and harvested by scraping. Genomic DNA was extracted using the GeneJET genomic DNA purification Kit (Thermo Scientific #K0721) according to the manufacturer's instructions.

To determine mitochondrial DNA integrity, a PCR reaction was performed on gDNA samples using 6 ng of template gDNA, 250 µM dNTPs, 500 nM of either a short read (tRNA(LEU)) or a long read (LR-mtDNA) primer mix, 0.02U/µl Q5 DNA polymerase and 1X Q5 reaction buffer. Long read PCR was aided by the addition of 10 ng/µl BSA. PCR products were then run on a 0.8% agarose gel, and quantified using Fiji software as described for immunoblots.

RNA extraction.

7 x10^6 cells were harvested by scraping into 0.2 ml of media, 1 ml TRI-reagent was added and the samples incubated (5 minutes at RT). 200 µl 1-Bromo-3-chloropropane (BCP; 11.76% (v/v) in TRI reagent and residual DMEM) was then added and the sample incubated for a further 3 minutes at RT before centrifugation (10,000 x g, Labnet, Prism R). The upper (colourless) layer was removed and incubated overnight at -20^{O}C in acidifed isopropanol solution (256 mM sodium acetate pH 4 and 36% isopropanol (v/v)). Samples were centrifuged at 17,000 x g for 15 minutes at 4^{O}C and pellets washed in 70% ethanol. Samples were DNase treated with RNAse free DNase-I (Qiagen) according to the manufacturer's instructions. RNA was isolated by phenol-chloroform-isoamyl-alchohol (50% phenol-chloroform-isoamy alchohol (v/v) 125:24:1 in dH_2O. Samples were vigorously shaken and incubated for 3 minutes at RT before centrifugation. The upper aqueous phase was transferred to a fresh tube and incubated overnight at -20 ^{O}C in acidified ethanol solution (323mM sodium acetate pH 5.2 and 65% ethanol (v/v)). Precipitated samples were washed in 70% ethanol, pellets dried, dissolved in dH_2O and RNA concentration determined by spectrophotometry (Nanodrop 2000, Thermo Scientific).

Comparative qPCR.

qPCR was performed using iTaq^{TM} Universal SYBR$^®$ Green Supermix (BIORAD) as per the manufacturer's instructions on a qPCR thermocycler (7500 fast real-time qPCR, Applied Biosciences). gDNA samples were analysed at a final concentration of 200 pg/µl with 500 nM primers (see Table S2). Data sets were analysed, and reference genes verified using the Pfaffl method (Pfaffl, no date) and REST software (QIAGEN).

Subcellular fractionation

Cells grown to 80-90% confluence in 15 cm^2 petri dishes were washed and scraped into PBS and pelleted at 300 g for 3 minutes, before re-suspension in 2ml homogenisation buffer (200 mM Mannitol, 70 mM Sucrose, 1 mM EGTA, 10 mM HEPES, pH 7.5) supplemented with protease and kinase inhibitors. Lysates were prepared in a glass homogeniser (Teflon), a sample taken as whole cell extract, before spinning at 1000 g, 4°C for 5 minutes. Supernatants were transferred to a fresh tube (mitochondrial/cytoplasmic fraction) and centrifuged at 10,000 g, 4°C for 15 minutes to pellet mitochondria before re-suspension in homogenisation buffer.

Protein concentration was then measured by Bradford assay and samples were boiled in SDS sample buffer, and 20 µg protein loaded onto an SDS-page gel for analysis.

Resazurin assays.

Mitochondrial metabolism assays were performed using 20 µg of isolated mitochondria were re-suspended in Locke's buffer (154 mM NaCl, 5.6 mM KCl (BDH), 2.3 mM $CaCl_2$ (Fischer), 1 mM $MgCl_2$, 3.6 mM $NaHCO_3$, 5 mM Glucose and 5 mM HEPES pH 7.5 (BDH) and plated into 1 well of a black 96 well plate (CLS3904). 40 µM resazurin was then added to each sample to make a final concentration of 20 µM and plates were then incubated at 37°C with 5% CO_2. Absorbance was then read at 595nm every 30 minutes for 4 h and compared to that of 20 µM resazurin blank controls (FluoStar Galaxy).

Cell death curves were performed on 50,000 HeLa cells expressing GFP, pre-treated with and without 1 µM of the BCL-2 inhibitor Navitoclax for 16h. Cells were treated with 0, 0.02, 0.08, 0.32, 1.28 or 2.56 J of UV, left for 24 h, 20 µM of resazurin added and plates incubated at 37°C with 5% CO_2 for 1h. Absorbance was read at 595nm and compared to 20 µM resazurin control.

Glucose-Glo and Lactate-Glo assay.

10,000 HeLa cells were plated per well of a 96 well plate in 100 µl DMEM (Gibco 11054001) containing 5.6 mM glucose, 2 mM glutamine and supplemented with 10% FCS. Media only wells acted as controls. At 8, 24, 48 and 72 h post plating, 2.5 µl of media was removed from each sample, diluted in 97.5 µl of PBS and frozen until needed. On day of assay, samples thawed and were diluted a further 2.5 x, and 50 µl of diluted media added to a white 96 well plate (CLS3610) before the addition of 50 µl of Lactate/Glucose detection reagent (Promega). Plates were incubated for 1 h at RT and luminescence recorded (Glowmax Luminometer, Promega) and then compared to Glucose/Lactate standards to determine relevant concentrations.

Live Cell Fluorescence imaging.

To visualise active mitochondria, cells were grown overnight in 8-chambered micro-slides (Ibidi). Cells were stained to visualise mitochondria using either 500 nM MitoTracker Red CMXRos, MitoTracker Deep Red FM or 200nM MitoTracker Green FM (Invitrogen), and Nucblue to visualise DNA (Thermo Fischer Scientific) in phenol-red free CO_2 independent media (DMEM, Invitrogen) supplemented with 2 mM L-glutamine and 10% Fetal Calf Serum, for 15 minutes at 37°C.

Mitochondrial membrane potential assay.

HeLa or MRC5 cells were seeded into Ibidi 8-chambered chambers approximately 24 h before imaging and once adherent, were incubated in DMEM without phenol red (D1145) supplemented with 4 mM L-glutamine and 25 mM HEPES. 15 minutes before imaging, cells were stained with 1 drop of Nucblue (Life Technologies), 100 nM MitoTracker Green FM and 100 nM MitoTracker Deep Red FM or 200 µM

tetramethylrhodamine ethyl ester perchlorate (TMRE, AAT Bioquest). Immediately before imaging, stains were washed off by replacing media with phenol red free CO_2 –independent complete DMEM.

Image acquisition and processing.

Imaging was performed using an inverted (DMRIB Olympus, Delta Vision Elite) microscope with a 60x (NA1.4, oil) objective. Single plane images were acquired, de-convolved using inbuilt software on the Delta-vision and saved as TIFF files. Image pixel intensity was quantified in Fiji using a fully automated macro, which was programmed first to threshold each channel to a set scale defined by the user, and then measure the average signal intensity of each channel. Co-localisation analysis was performed using a similar macro that after thresholding images, was then programmed to analyse the percentages of pixels that spatially co-localised with similar intensity between the two channels. Datasets were then analysed in the GraphPad Prism software.

Figure Legends.

Figure 1. Survivin up-regulation increases mitochondrial mass independent of altered mitochondrial biogenesis or dynamics **(A)** Immunoblot of the mitochondria enriched fractions (Mito) from GFP and survivin-GFP (SVN-GFP) overexpressing MRC5, HeLa and U2OS cells. Whole cell extracts (WCE) are included in the lower panel to indicate equality in expression of each ectopic protein. VDAC is a mitochondrial (OMM) marker; Histone 3 indicates any nuclear contamination, and tubulin serves both an indicator of cytoplasmic contamination (Mito) and a loading control (WCE). **(B-E)** Immunoblot analysis of VDAC protein expression in WCEs from HeLa sublines indicated, probed with tubulin as a loading control. Compared to GFP controls SVN-GFP expressing cells had increased VDAC expression. **(C)** Semi-quantitative analysis of (B). Pixel intensity was normalised to tubulin, and presented as fold change (Log2 scale) compared to the GFP control. Two-way ANOVA used to test significance, $p<0.01$ (**). **(D)** Experiment described in (B) carried out in MRC5 cells. **(E)** Semi-quantitative analysis of immunoblot in (D) normalised to tubulin. Pixel intensity quantified as described above (C). Two-way ANOVA shows no statistical differences in protein expression caused by SVN-GFP expression. All error bars indicate +/- SEM, N=3 (triplicate). **(F)** qPCR analysis of VDAC expression in HeLa cells over-expressing GFP or SVN-GFP. VDAC mRNA remains constant with SVN-GFP expression. **(G-H)** mtDNA copy number was determined by qPCR analysis on genomic DNA extracted from **(G)** HeLa and **(H)** MRC5 cells expressing GFP or SVN-GFP. The mitochondrial encoded tRNA(LEU) gene was quantified and compared to two stably expressed nuclear reference genes, tubulin (TUBB) and actin (ACTB) or GAPDH. tRNA(LEU) was increased and decreased in SVN-GFP expressing HeLas and MRC5 cells respectively $p<0.0001$ (****). **(I)** Immunoblotting of WCE's from HeLa or **(K)** MRC5 cells over-expressing GFP or SVN-GFP. Membranes were probed for PGC1α as a mitochondrial biogenesis marker and tubulin as a loading control, N=3 (with internal triplicates). **(J)** and **(L)** Semi-quantification of immunoblots in (I) and (K) respectively, presented as fold change (Log2 scale) compared to the GFP control**.** TWO-way ANOVA shows SVN-GFP expression in HeLa cells reduces the expression of PGC1α but causes no alterations in MRC5 cells, $p<0.0001$ (****). **(M-N)** HeLa cells expressing GFP or SVN-GFP were stained with 250 nM MitoTracker Red FM and imaged live: 3 mitochondrial phenotypes were observed; normal, intermediate or fragmented. Chi-squared test indicated a similar mitochondrial distribution in both lines regardless of survivin status, N=3, DF=2. Full galleries are shown in supplementary Figures S2. **(O-P)** HeLa cells transiently expressing RFP or SVN-RFP were stained with MitoTracker Green (MTG) or MitoTracker Far Red (MTFR) and imaged live. Images were thresholded using Fiji software, mean pixel intensity and area was quantified and MTFR signal normalised to MTG. TWO-way ANOVA analysis shows survivin overexpression does not alter mitochondrial membrane potential in HeLa cells but does increase mitochondrial pixel area, $p<0.0001$(****), N=3.

Figure 2. Mitochondrial localisation of survivin is required for mitochondrial mass alterations **(A)** MRC5 cells expressing GFP, SVN-GFP or MTS-survivin-GFP (MTS-SVN-GFP) were stained with 250 nM MitoTracker Red FM and NucBlue, then imaged live to prove MTS-SVN-GFP forces the mitochondrial localisation of survivin in non-

cancerous normal fibroblasts. **(B)** Immunoblot analysis of PGC1α and VDAC protein expression in WCEs from MRC5 sublines indicated, probed with tubulin as a loading control. Compared to GFP controls MTS-SVN-GFP expressing cells had increased VDAC expression, and showed no alterations to PGC1α expression. **(C-D)** Semi-quantitative analysis of (B). Pixel intensity of each respective protein was normalised to tubulin, and presented as fold change (Log2 scale) compared to the GFP control. Two-way ANOVA used to test significance, $p<0.001$ (***).

Figure 3. Survivin does not interfere with mitophagic stages preceding Parkin mitochondrial translocation. **(A** and **B)** HeLa cells were treated with 10 µM FCCP for 6 h, stained with 250 nM MitoTracker Red and imaged live. Mitochondrial distribution was scored as normal, fragmented, or intermediate, and no significant difference between cells expressing GFP or SVN-GFP was seen (Chi-squared test, N=3, DF=2). **(C)** HeLa cells transiently transfected with cDNA for RFP or SVN-RFP were treated as in (A) and mitochondrial membrane potential measured using MitoTracker far red, and expressed as a ratio to MTG. SVN-GFP expression did not alter MitoTracker Deep Red signal intensity, indicating no alterations to mitochondrial membrane potential. (**D, F** and **H)** HeLa, U2OS and MRC5 cells were treated with 10 µM FCCP for 6, 12 and 24 hrs, WCEs prepared and analysed by immunoblotting. Membranes were probed for expression of the kinase PINK1, GFP to confirm cell line expression and tubulin used as a loading control, N=3 (with internal triplicates). SVN-GFP expression does not alter PINK1 stabilisation post mitophagy stimulation. (**E, G** and **I)** Semi-quantification of immunoblots in **(D, F** and **H)** respectively, presented as fold change (Log_2 scale) compared to the GFP control time 0. Error bars represent +/- SEM N=3 DF=32 (with internal triplicates). No statistical alterations are observed (TWO-way ANOVA). **(J)** GST-pull down assay of purified GST-Parkin and GST alone using WCE made from HeLa GFP or SVN-GFP cells. Samples were analysed by immunoblotting, and membranes probed for GST to confirm pulldown, GFP to check expression in WCE's, and PINK1 to assess success of pulldown. Tubulin was used as a loading control. SVN-GFP does not prevent the interaction of GST-Parkin with PINK1. N=3.

Figure 4. Survivin prevents mitochondrial recruitment of mCherry-Parkin. **(A)** HeLa or **(C)** MRC5 cells were treated with 10 µM FCCP post-transfection with cDNA encoding mCherry-Parkin and stained with NucBlue to visualise nuclei. Representative images, thresholded using Fiji software, scale bars 15 µm. Full MRC5 figure shown in Figure S3 **(B and C)** Cells were counted for mitochondrial or cytoplasmic localisation of mCherry-Parkin, and a Chi-squared test performed to analyse differences in phenotypes. **(B)** In HeLa cells, Parkin relocates to the mitochondria in GFP cells treated with FCCP, but remains cytoplasmic in SVN-GFP cells, $p<0.0001$ (****) N=3. **(C)** No alterations were observed in mCherry-Parkin translocation in MRC5 cells (P-value 0.6748 and 0.4112, N=3).

Figure 5. Mitochondrial co-localisation with lysosomes is reduced in survivin-RFP expressing HeLa cells. **(A)** HeLa cells were treated with 10 µM FCCP post-transfection with cDNA encoding RFP or survivin-RFP and stained with 75nM LysoTracker Blue to visualise lysosomes and 250nM MitoTracker Green for mitochondria. Representative images, thresholded using Fiji Software, scale bars

15µm. Expanded sections to show co-localisation of mitochondria and lysosomes. Full figure shown in Figure S4. **(B and C)** Pixel intensity profile plots over a line draw through a section of RFP **(B)** and survivin-RFP **(C)** cells treated with FCCP. RFP cells show a co-localisation of LysoTracker Blue and MitoTracker Green peaks. **(D)** Fiji co-localisation analysis of MitoTracker Green and LysoTracker Blue pixels, shown as percentage co-localisation. ONE-way ANOVA analysis shows significant increase in co-localisation after FCCP treatment of RFP cells, but no alteration to survivin-RFP cells, p<0.0001 (****), N=3. Error bars mean +/- SEM.

Figure 6. mtDNA quality decreases in HeLa cells over-expressing survivin **(A**, **C** and **E)** Long read (9 kb) and short read (150 bp) PCR products derived from genomic DNA extracted from **(A)** HeLa cells expressing GFP or SVN-GFP, or survivin knockdown with siRNA (SVN siRNA) **(C)**, also in normal fibroblast MRC5 cells **(E)**. Long read fragments were reduced in survivin-GFP expressing HeLas, but increased after SVN siRNA. In comparison, in MRC5 cells no change was observed after survivin depletion. **(B, D** and **F)** Semi-quantitative analysis of the long read band intensity normalised to the short read 150 bp product**.** Statistical significance was determined using Two-way ANOVA, p<0.001 (***) p<0.0001 (****), error bars mean +/- SEM N=3 (triplicate).

Figure 7. Effect of chloroquine (CQ) treatment on mitochondrial respiration. Mitochondria isolated from **(A** and **B)** HeLa **(C** and **D)** U2OS or MRC5 **(E** and **F)** cells expressing GFP or SVN-GFP were plated with the addition of resazurin media +/- 50 µM or 150 µM CQ and metabolism measured by produced resorufin absorption, measured in relative fluorescence units (RFU) every 30 minutes for 4 h. Data was plotted as a curved graph (A, C and E), and analysed to calculate the fold change (Log2) in resorufin absorbance compared to GFP control (B, D and F). Non-linear regression shows no line fits between GFP curves in HeLa **(A)** or U2OS **(C)** mitochondria, whereas no change or a statistical increase is seen in SVN-GFP cells treated in response to CQ treatment (p<0.001, or p=0.1405 and 0.4825 respectively). **(B** and **D)** Two-way ANOVA reveals mitochondria isolated from GFP expressing HeLa and U2OS cells display a greater negative fold change in resorufin absorbance post chloroquine treatment compared to SVN-GFP mitochondria, p<0.0001 (****). **(E** and **F)** Mitochondrial isolated from MRC5 expressing GFP or SVN-GFP display the same fold change in resorufin fluorescence post-CQ treatment (F). Non-linear regression analysis shows line fits both MRC5 GFP and SVN-GFP 50 µM or 150 µM CQ (E). Error bars represent mean +/- SEM, N=3 (triplicate).

Figure 8. Analysis of mitochondrial respiration, response to oligomycin and lactate production. Mitochondria were isolated from **(A** and **B)** HeLa, **(C** and **D)** U2OS or **(E)** MRC5 cells expressing GFP or SVN-GFP and plated in resazurin medium with or without oligomycin and metabolism assessed by produced resorufin absorbance, measured in relative fluorescence units (RFU) every 30 minutes for 4 h. Data was plotted as a curved graph (A, C and E), and analysed to calculate the fold change (Log2) in resorufin absorbance compared to GFP control (B and D). Non-linear regression analysis demonstrates oligomycin treatment significantly alters GFP metabolism in **(A)** and **(C),** p<0.001 (***), p<0.0001 (****), whereas significantly less

in SVN-GFP. A single curve fitted all datasets in **(E)**; GFP vs SVN-GFP, GFP + oligomycin and SVN-GFP + oligomycin (p=0.9808 and 0.4123 respectively). **(B** and **D)** Non-linear regression analysis reveals mitochondria from HeLa and U2OS display a greater fold change in resorufin fluorescence with oligomycin treatment compared to SVN-GFP mitochondria, p<0.001 (***), p<0.0001 (****). **(F)** Mitochondria isolated from MRC5 cells expressing GFP, SVN-GFP or MTS-SVN-GFP were metabolically analysed as mentioned previously. Non-linear regression analysis demonstrates that MTS-SVN-GFP expression reduces resorufin fluorescence in comparison to GFP or SVN-GFP, p<0.0001 (****) **(G)** Glucose consumption of 10,000 cells was measured over 72 h using a glucose-Glo assay. Two-way ANOVA test at 24h was used to determine significance, p<0.01 (**). Regression analysis to analyse difference in rate of change, F test proves significant difference (p=0.0176). **(H)** Lactate production was measured as for **(G)** using a lactate-Glo assay. Two-way ANOVA test at 24h was used to determine significance p<0.001 (***). Regression analysis and F-test proves significant differences (p=0.0029). Dotted line shows glucose or lactate concentration at 0h. Error bars represent mean +/- SEM, N=2 (internally in triplicate). **(I)** HeLa cells expressing GFP and SVN-GFP grow at the same rate. 200 HeLa cells were seeded and the number of cells per colony counted over 72 h. Error bars represent mean +/- SEM, N=3 (internally in triplicate).

Acknowledgements.
We thank Dr. Sophie Rochette for technical support, Alex Fezovich for generating the MTS-survivin cell lines and his assistance with FiJi, James Grey for his expertise in qPCR data acquisition and analysis, and Prof. Seamus Martin for mCherry-PARKIN. A.Townley is a BBSRC-DTP funded student, we thank the BBSRC for her support.

References.

Balaban, R. S., Nemoto, S. and Finkel, T. (2005) 'Mitochondria, Oxidants, and Aging', *Cell*, 120(4), pp. 483–495. doi: 10.1016/j.cell.2005.02.001.

Barrett, R. M. A., Osborne, T. P. and Wheatley, S. P. (2009) 'Phosphorylation of survivin at threonine 34 inhibits its mitotic function and enhances its cytoprotective activity', *Cell Cycle*, 8(2), pp. 278–283. doi: 10.4161/cc.8.2.7587.

Carvalho, A., Carmena, M., Sambade, C., Earnshaw, W. C. and Wheatley, S. P. (2003) 'Survivin is required for stable checkpoint activation in taxol-treated HeLa cells.', *Journal of cell science*. The Company of Biologists Ltd, 116(Pt 14), pp. 2987–98. doi: 10.1242/jcs.00612.

Chatterjee, A., Dasgupta, S. and Sidransky, D. (2011) 'Mitochondrial subversion in cancer.', *Cancer prevention research (Philadelphia, Pa.)*. NIH Public Access, 4(5), pp. 638–54. doi: 10.1158/1940-6207.CAPR-10-0326.

Chourasia, A. H., Boland, M. L. and Macleod, K. F. (2015) 'Mitophagy and cancer', *Cancer & Metabolism*. BioMed Central, 3(1), p. 4. doi: 10.1186/s40170-015-0130-8.

Colnaghi, R., Connell, C. M., Barrett, R. M. A. and Wheatley, S. P. (2006) 'Separating the Anti-apoptotic and Mitotic Roles of Survivin', *Journal of Biological Chemistry*. American Society for Biochemistry and Molecular Biology, 281(44), pp. 33450–33456. doi: 10.1074/jbc.C600164200.

Dispersyn, G., Nuydens, R., Connors, R., Borgers, M. and Geerts, H. (1999) 'Bcl-2 protects against FCCP-induced apoptosis and mitochondrial membrane potential depolarization in PC12 cells', *Biochimica et Biophysica Acta (BBA) - General Subjects*. Elsevier, 1428(2–3), pp. 357–371. doi: 10.1016/S0304-4165(99)00073-2.

Dohi, T., Beltrami, E., Wall, N. R., Plescia, J. and Altieri, D. C. (2004) 'Mitochondrial survivin inhibits apoptosis and promotes tumorigenesis', *Journal of Clinical Investigation*, 114(8), pp. 1117–1127. doi: 10.1172/JCI200422222.

Dohi, T., Xia, F. and Altieri, D. C. (2007) 'Compartmentalized phosphorylation of IAP by protein kinase A regulates cytoprotection.', *Molecular cell*. NIH Public Access, 27(1), pp. 17–28. doi: 10.1016/j.molcel.2007.06.004.

East, D. A. and Campanella, M. (2016) 'Mitophagy and the therapeutic clearance of damaged mitochondria for neuroprotection', *The International Journal of Biochemistry & Cell Biology*, 79, pp. 382–387. doi: 10.1016/j.biocel.2016.08.019.

Elmore, S. P., Qian, T., Grissom, S. F. and Lemasters, J. J. (2001) 'The mitochondrial permeability transition initiates autophagy in rat hepatocytes.', *FASEB journal : official publication of the Federation of American Societies for Experimental Biology*. Federation of American Societies for Experimental Biology, 15(12), pp. 2286–7. doi: 10.1096/fj.01-0206fje.

Engelsma, D., Rodriguez, J. A., Fish, A., Giaccone, G. and Fornerod, M. (2007) 'Homodimerization Antagonizes Nuclear Export of Survivin', *Traffic*. John Wiley & Sons, Ltd (10.1111), 8(11), pp. 1495–1502. doi: 10.1111/j.1600-0854.2007.00629.x.

Escuín, D. and Rosell, R. (1999) 'The Anti-Apoptosis Survivin Gene and its Role in Human Cancer: An Overview', *Clinical Lung Cancer*. Elsevier, 1(2), pp. 138–143. doi: 10.3816/CLC.1999.n.011.

Fortugno, P., Wall, N. R., Giodini, A., O'Connor, D. S., Plescia, J., Padgett, K. M., Tognin, S., Marchisio, P. C. and Altieri, D. C. (2002) 'Survivin exists in

immunochemically distinct subcellular pools and is involved in spindle microtubule function.', *Journal of cell science*, 115(Pt 3), pp. 575–85. Available at: http://www.ncbi.nlm.nih.gov/pubmed/11861764 (Accessed: 23 April 2019).
van Gisbergen, M. W., Voets, A. M., Starmans, M. H. W., de Coo, I. F. M., Yadak, R., Hoffmann, R. F., Boutros, P. C., Smeets, H. J. M., Dubois, L. and Lambin, P. (2015) 'How do changes in the mtDNA and mitochondrial dysfunction influence cancer and cancer therapy? Challenges, opportunities and models', *Mutation Research/Reviews in Mutation Research*. Elsevier, 764, pp. 16–30. doi: 10.1016/J.MRREV.2015.01.001.
Hagenbuchner, J., Kiechl-Kohlendorfer, U., Obexer, P. and Ausserlechner, M. (2016) 'BIRC5/Survivin as a target for glycolysis inhibition in high-stage neuroblastoma', *Oncogene*, 35, pp. 2052–2061. doi: 10.1038/onc.2015.264.
Hagenbuchner, J., Kuznetsov, A. V, Obexer, P. and Ausserlechner, M. J. (2013) 'BIRC5/Survivin enhances aerobic glycolysis and drug resistance by altered regulation of the mitochondrial fusion/fission machinery.', *Oncogene*. Nature Publishing Group, 32(40), pp. 4748–57. doi: 10.1038/onc.2012.500.
Hollville, E., Carroll, R. G., Cullen, S. P. and Martin, S. J. (2014) 'Bcl-2 Family Proteins Participate in Mitochondrial Quality Control by Regulating Parkin/PINK1-Dependent Mitophagy', *Molecular Cell*. Elsevier, 55(3), pp. 451–466. doi: 10.1016/J.MOLCEL.2014.06.001.
Humphry, N. J. and Wheatley, S. P. (2018) 'Survivin inhibits excessive autophagy in cancer cells but does so independently of its interaction with LC3.', *Biology open*. The Company of Biologists Ltd, 7(10), p. bio037374. doi: 10.1242/bio.037374.
Jaiswal, P. K., Goel, A. and Mittal, R. D. (2015) 'Survivin: A molecular biomarker in cancer.', *The Indian journal of medical research*. Wolters Kluwer -- Medknow Publications, 141(4), pp. 389–97. doi: 10.4103/0971-5916.159250.
Jornayvaz, F. R. and Shulman, G. I. (2010) 'Regulation of mitochondrial biogenesis.', *Essays in biochemistry*. NIH Public Access, 47, pp. 69–84. doi: 10.1042/bse0470069.
Kazlauskaite, A., Kondapalli, C., Gourlay, R., Campbell, D. G., Ritorto, M. S., Hofmann, K., Alessi, D. R., Knebel, A., Trost, M. and Muqit, M. M. K. (2014) 'Parkin is activated by PINK1-dependent phosphorylation of ubiquitin at Ser ^{65}', *Biochemical Journal*, 460(1), pp. 127–141. doi: 10.1042/BJ20140334.
Lee, J.-Y., Nagano, Y., Taylor, J. P., Lim, K. L. and Yao, T.-P. (2010) 'Disease-causing mutations in parkin impair mitochondrial ubiquitination, aggregation, and HDAC6-dependent mitophagy.', *The Journal of cell biology*. The Rockefeller University Press, 189(4), pp. 671–9. doi: 10.1083/jcb.201001039.
Matthew G. Vander Heiden, L. C. C. C. B. T. (2009) 'Understanding the Warburg Effect: The Metabolic Requirements of Cell Proliferation', *Science (New York, N.Y.)*. NIH Public Access, 324(5930), p. 1029.
Merz, S. and Westermann, B. (2009) 'Genome-wide deletion mutant analysis reveals genes required for respiratory growth, mitochondrial genome maintenance and mitochondrial protein synthesis in Saccharomyces cerevisiae.', *Genome biology*. BioMed Central, 10(9), p. R95. doi: 10.1186/gb-2009-10-9-r95.
Morrison, D. J., Hogan, L. E., Condos, G., Bhatla, T., Germino, N., Moskowitz, N. P., Lee, L., Bhojwani, D., Horton, T. M., Belitskaya-Levy, I., Greenberger, L. M., Horak, I. D., Grupp, S. A., Teachey, D. T., Raetz, E. A. and Carroll, W. L. (2012) 'Endogenous knockdown of survivin improves chemotherapeutic response in ALL models.', *Leukemia*. NIH Public Access, 26(2), pp. 271–9. doi: 10.1038/leu.2011.199.

Nicholls, D. G. (2004) 'Mitochondrial membrane potential and aging.', *Aging cell*, 3(1), pp. 35–40. Available at: http://www.ncbi.nlm.nih.gov/pubmed/14965354 (Accessed: 3 July 2017).
Nunnari, J., Marshall, W. F., Straight, A., Murray, A., Sedat, J. W. and Walter, P. (1997) 'Mitochondrial transmission during mating in Saccharomyces cerevisiae is determined by mitochondrial fusion and fission and the intramitochondrial segregation of mitochondrial DNA.', *Molecular biology of the cell*. American Society for Cell Biology, 8(7), pp. 1233–42. Available at: http://www.ncbi.nlm.nih.gov/pubmed/9243504 (Accessed: 21 June 2017).
Ott, M., Gogvadze, V., Orrenius, S. and Zhivotovsky, B. (2007) 'Mitochondria, oxidative stress and cell death', *Apoptosis*, 12, pp. 913–922. doi: 10.1007/s10495-007-0756-2.
Palikaras, K., Lionaki, E. and Tavernarakis, N. (2015) 'Balancing mitochondrial biogenesis and mitophagy to maintain energy metabolism homeostasis', *Cell Death & Differentiation*, 22(9), pp. 1399–1401. doi: 10.1038/cdd.2015.86.
Pfaffl, M. W. (no date) *Relative quantification*. Available at: https://gene-quantification.de/pfaffl-rel-quan-book-ch3.pdf (Accessed: 28 August 2018).
Porporato, P. E., Filigheddu, N., Pedro, J. M. B.-S., Kroemer, G. and Galluzzi, L. (2017) 'Mitochondrial metabolism and cancer', *Cell Research*. Nature Publishing Group. doi: 10.1038/cr.2017.155.
Ray, P. D., Huang, B.-W. and Tsuji, Y. (2012) 'Reactive oxygen species (ROS) homeostasis and redox regulation in cellular signaling.', *Cellular signalling*. NIH Public Access, 24(5), pp. 981–90. doi: 10.1016/j.cellsig.2012.01.008.
Redmann, M., Benavides, G. A., Berryhill, T. F., Wani, W. Y., Ouyang, X., Johnson, M. S., Ravi, S., Barnes, S., Darley-Usmar, V. M. and Zhang, J. (2017) 'Inhibition of autophagy with bafilomycin and chloroquine decreases mitochondrial quality and bioenergetic function in primary neurons.', *Redox biology*. Elsevier, 11, pp. 73–81. doi: 10.1016/j.redox.2016.11.004.
Redmann, M., Dodson, M., Boyer-Guittaut, M., Darley-Usmar, V. and Zhang, J. (2014) 'Mitophagy mechanisms and role in human diseases.', *The international journal of biochemistry & cell biology*. NIH Public Access, 53, pp. 127–33. doi: 10.1016/j.biocel.2014.05.010.
Rivadeneira, D. B., Caino, M. C., Seo, J. H., Angelin, A., Wallace, D. C., Languino, L. R. and Altieri, D. C. (2015) 'Survivin promotes oxidative phosphorylation, subcellular mitochondrial repositioning, and tumor cell invasion.', *Science signaling*. NIH Public Access, 8(389), p. ra80. doi: 10.1126/scisignal.aab1624.
Sabharwal, S. S. and Schumacker, P. T. (2014) 'Mitochondrial ROS in cancer: initiators, amplifiers or an Achilles' heel?', *Nature Reviews Cancer*, 14(11), pp. 709–721. doi: 10.1038/nrc3803.
Shaid, S., Brandts, C. H., Serve, H. and Dikic, I. (2013) 'Ubiquitination and selective autophagy.', *Cell death and differentiation*. Nature Publishing Group, 20(1), pp. 21–30. doi: 10.1038/cdd.2012.72.
Stauber, R. H., Mann, W. and Knauer, S. K. (2007) 'Nuclear and cytoplasmic survivin: molecular mechanism, prognostic, and therapeutic potential.', *Cancer research*. American Association for Cancer Research, 67(13), pp. 5999–6002. doi: 10.1158/0008-5472.CAN-07-0494.
Sumpter, R., Sirasanagandla, S., Fernández, Á. F., Wei, Y., Dong, X., Franco, L., Zou,

Z., Marchal, C., Lee, M. Y., Clapp, D. W., Hanenberg, H., Levine, B. and Levine, B. (2016) 'Fanconi Anemia Proteins Function in Mitophagy and Immunity.', *Cell*. NIH Public Access, 165(4), pp. 867–81. doi: 10.1016/j.cell.2016.04.006.
Trempe, J.-F., Sauvé, V., Grenier, K., Seirafi, M., Tang, M. Y., Ménade, M., Al-Abdul-Wahid, S., Krett, J., Wong, K., Kozlov, G., Nagar, B., Fon, E. A. and Gehring, K. (2013) 'Structure of parkin reveals mechanisms for ubiquitin ligase activation.', *Science (New York, N.Y.)*. American Association for the Advancement of Science, 340(6139), pp. 1451–5. doi: 10.1126/science.1237908.
Twig, G., Elorza, A., Molina, A. J. A., Mohamed, H., Wikstrom, J. D., Walzer, G., Stiles, L., Haigh, S. E., Katz, S., Las, G., Alroy, J., Wu, M., Py, B. F., Yuan, J., Deeney, J. T., Corkey, B. E. and Shirihai, O. S. (2008) 'Fission and selective fusion govern mitochondrial segregation and elimination by autophagy', *The EMBO Journal*, 27(2), pp. 433–446. doi: 10.1038/sj.emboj.7601963.
Twig, G., Hyde, B. and Shirihai, O. S. (2008) 'Mitochondrial fusion, fission and autophagy as a quality control axis: the bioenergetic view.', *Biochimica et biophysica acta*, 1777(9), pp. 1092–7. doi: 10.1016/j.bbabio.2008.05.001.
Twig, G. and Shirihai, O. S. (2011) 'The interplay between mitochondrial dynamics and mitophagy.', *Antioxidants & redox signaling*. Mary Ann Liebert, Inc., 14(10), pp. 1939–51. doi: 10.1089/ars.2010.3779.
Vara-Perez, M., Felipe-Abrio, B. and Agostinis, P. (2019) 'Mitophagy in Cancer: A Tale of Adaptation', *Cells*. Multidisciplinary Digital Publishing Institute (MDPI), 8(5). doi: 10.3390/CELLS8050493.
Vives-Bauza, C., Zhou, C., Huang, Y., Cui, M., de Vries, R. L. A., Kim, J., May, J., Tocilescu, M. A., Liu, W., Ko, H. S., Magrané, J., Moore, D. J., Dawson, V. L., Grailhe, R., Dawson, T. M., Li, C., Tieu, K. and Przedborski, S. (2010) 'PINK1-dependent recruitment of Parkin to mitochondria in mitophagy.', *Proceedings of the National Academy of Sciences of the United States of America*. National Academy of Sciences, 107(1), pp. 378–83. doi: 10.1073/pnas.0911187107.
Warburg, O. (1956) 'On the Origin of Cancer Cells', *Science*. American Association for the Advancement of Science, 123(3191), pp. 235–314. doi: 10.1126/science.123.3191.309.
Westermann, B. (2010) 'Mitochondrial fusion and fission in cell life and death', *Nature Reviews Molecular Cell Biology*. Nature Publishing Group, 11(12), pp. 872–884. doi: 10.1038/nrm3013.
Wheatley, S. P. and Altieri, D. C. (2019) 'Survivin at a glance', *Journal of Cell Science*, 132(7), p. jcs223826. doi: 10.1242/jcs.223826.
Yadav, N. and Chandra, D. (2013) 'Mitochondrial DNA mutations and breast tumorigenesis.', *Biochimica et biophysica acta*. NIH Public Access, 1836(2), pp. 336–44. doi: 10.1016/j.bbcan.2013.10.002.
Youle, R. J. and Narendra, D. P. (2011) 'Mechanisms of mitophagy', *Nature Reviews Molecular Cell Biology*. Nature Publishing Group, 12(1), pp. 9–14. doi: 10.1038/nrm3028.
Zaffagnini, G. and Martens, S. (2016) 'Mechanisms of Selective Autophagy.', *Journal of molecular biology*. Elsevier, 428(9 Pt A), pp. 1714–24. doi: 10.1016/j.jmb.2016.02.004.

Figure 1
Townley and Wheatley, 2020

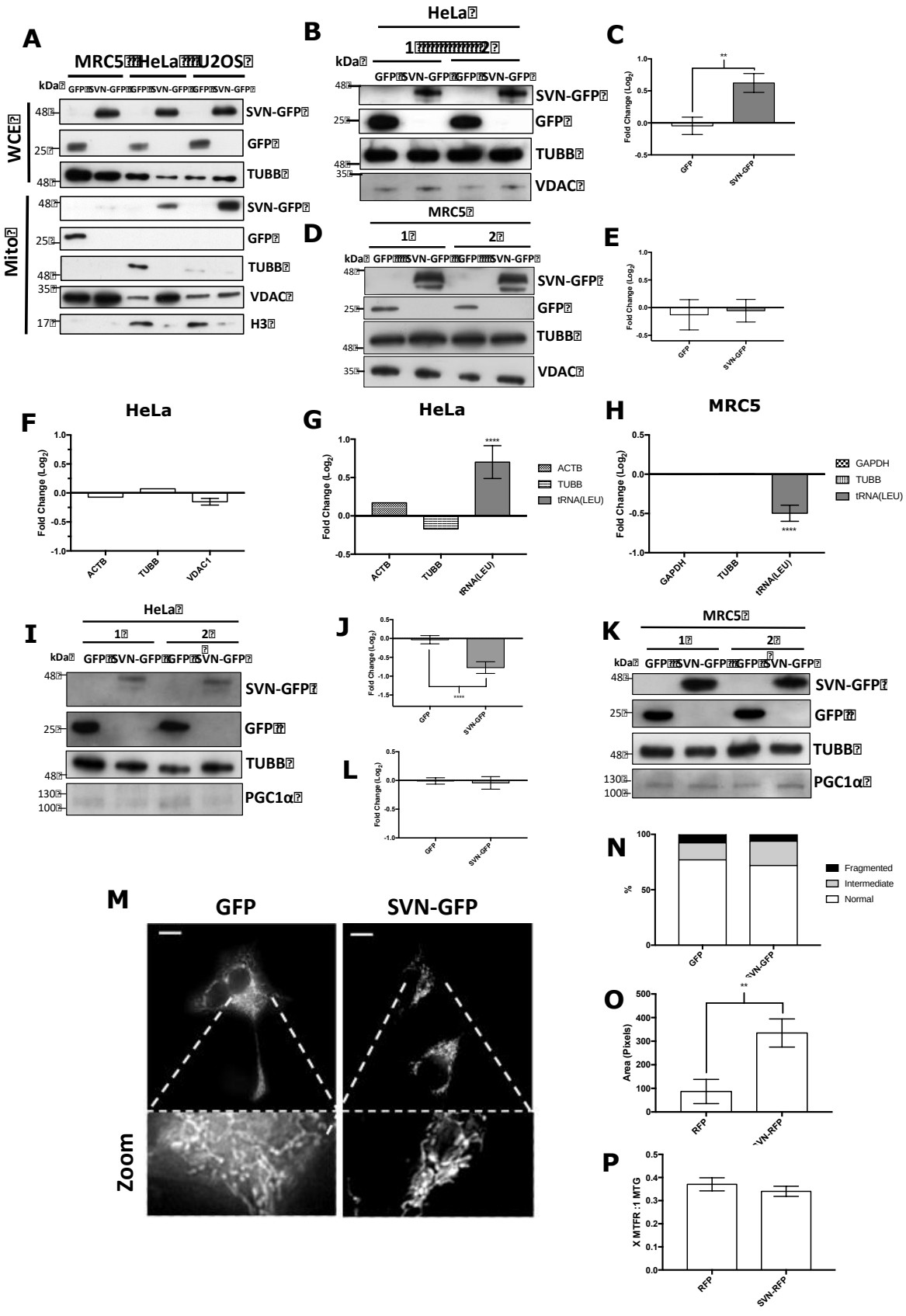

Figure 2
Townley and Wheatley, 2020

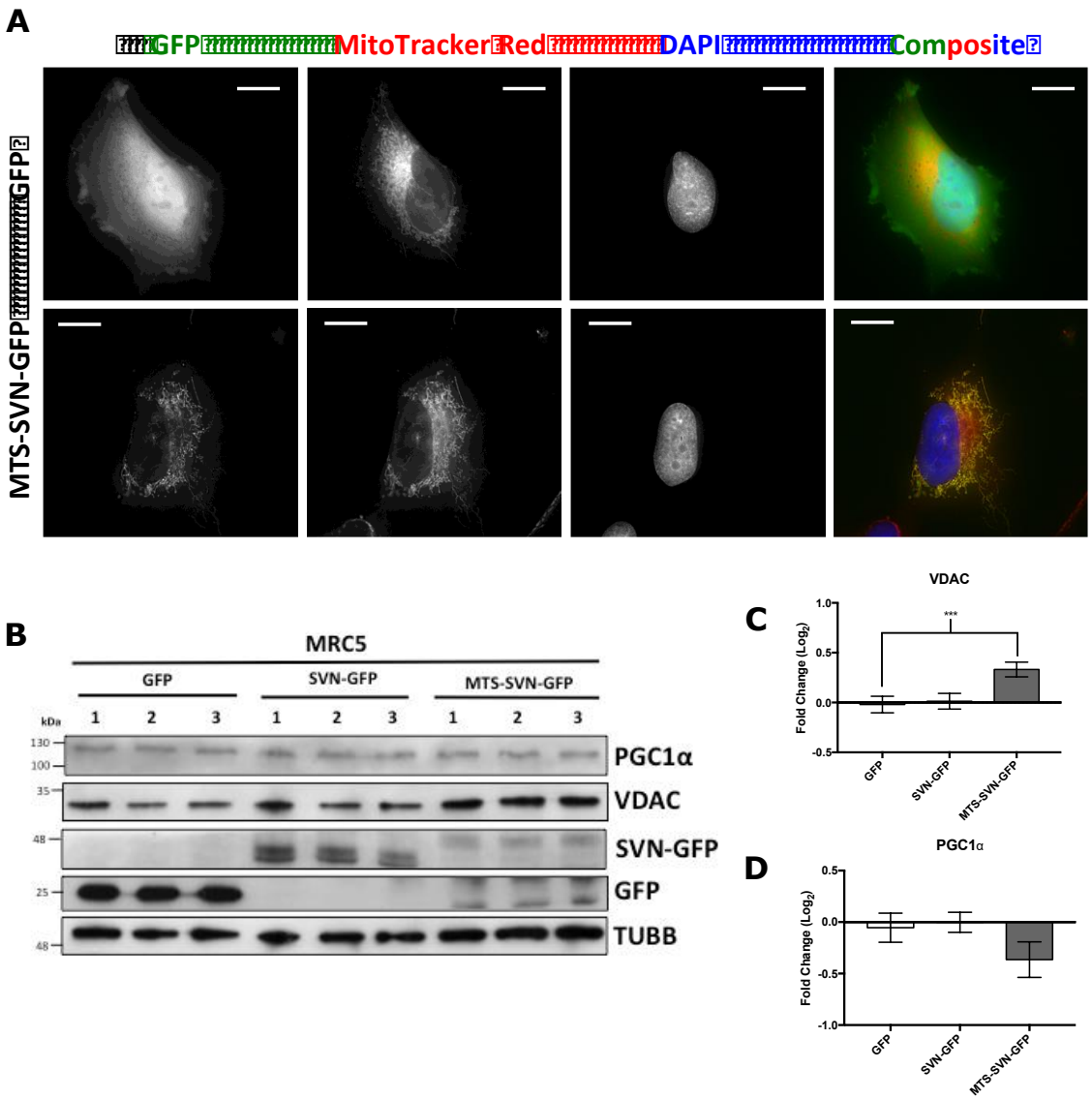

Figure 3
Townley and Wheatley, 2020

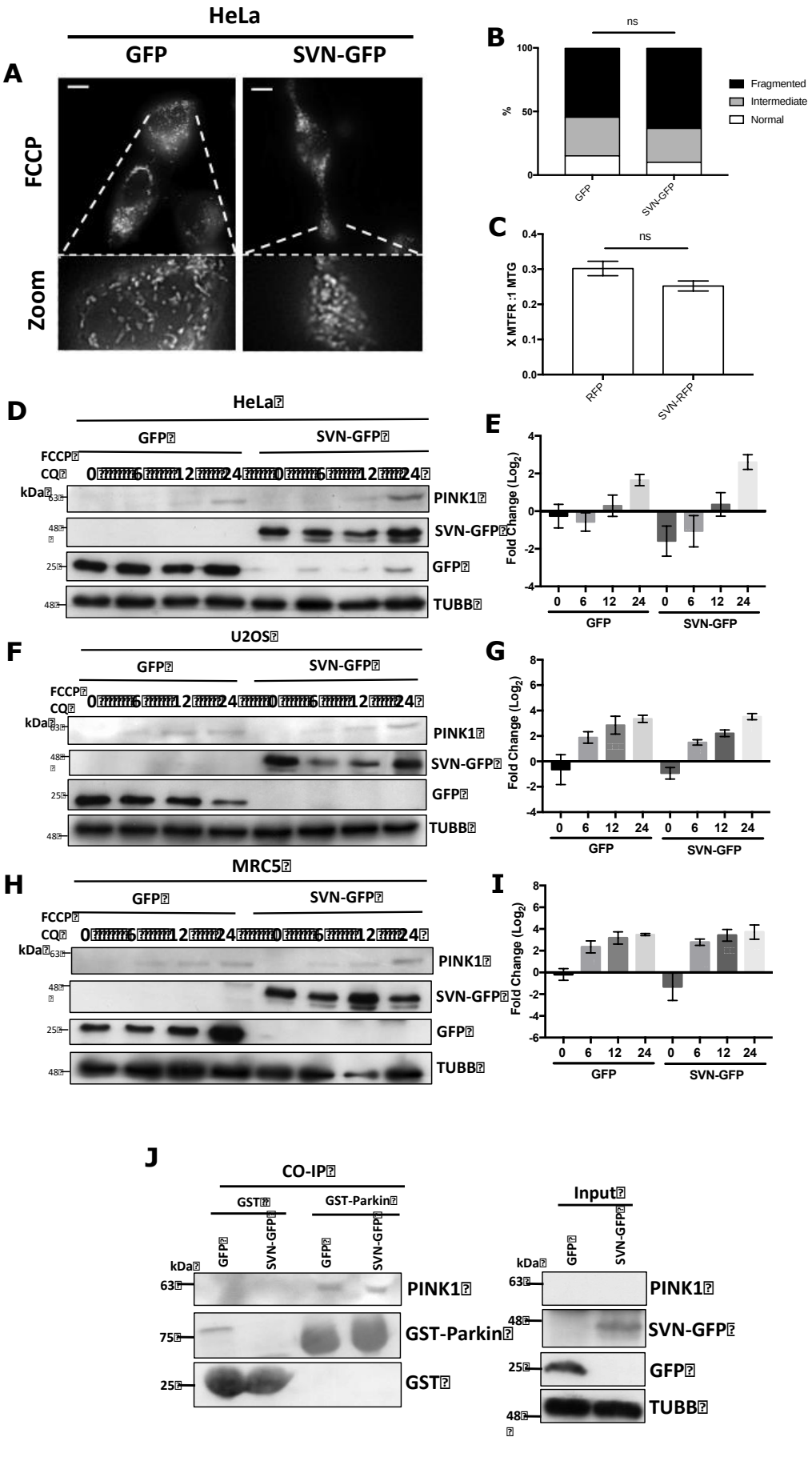

Figure 4
Townley and Wheatley, 2020

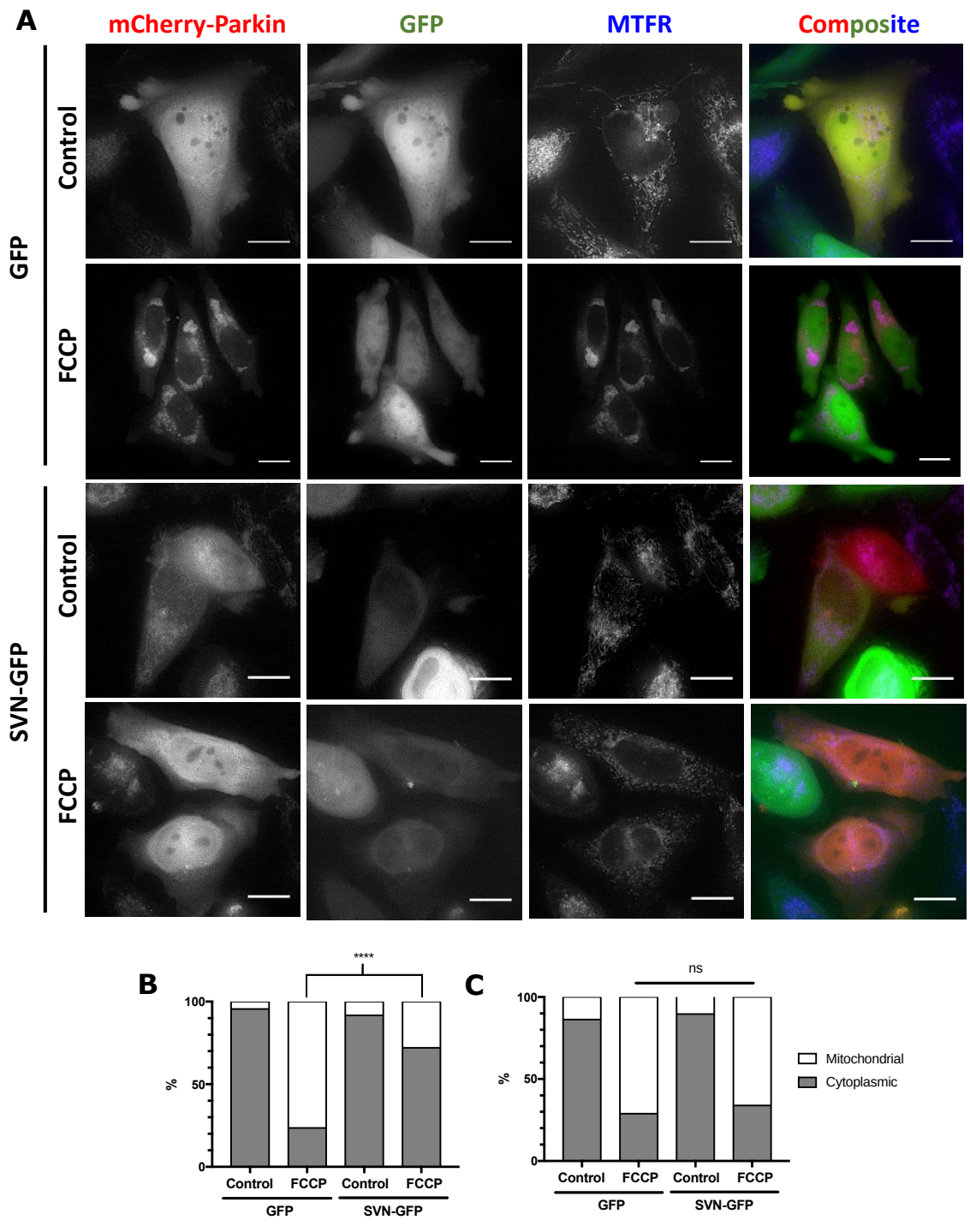

Figure 5
Townley and Wheatley, 2020

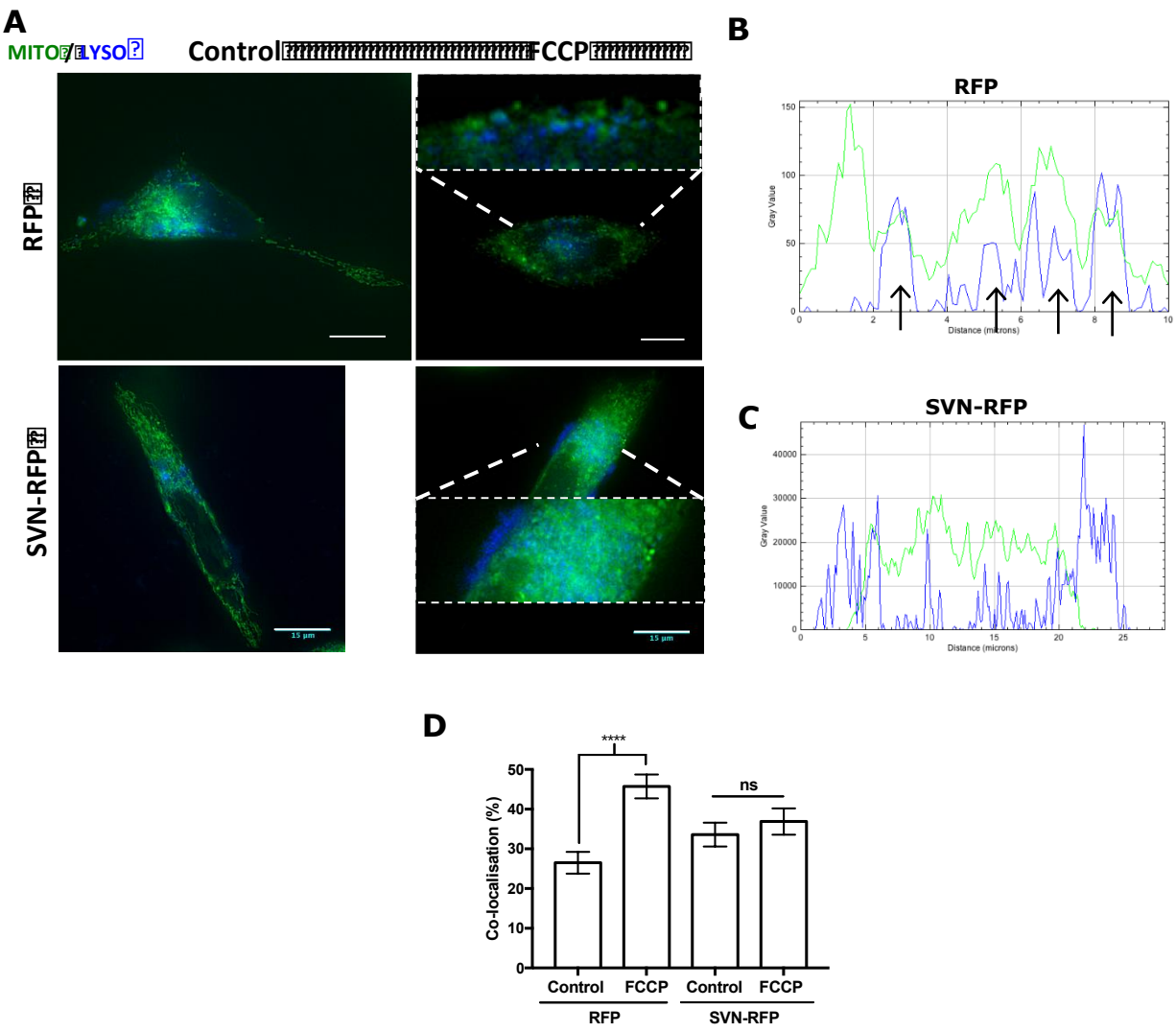

Figure 6
Townley and Wheatley, 2020

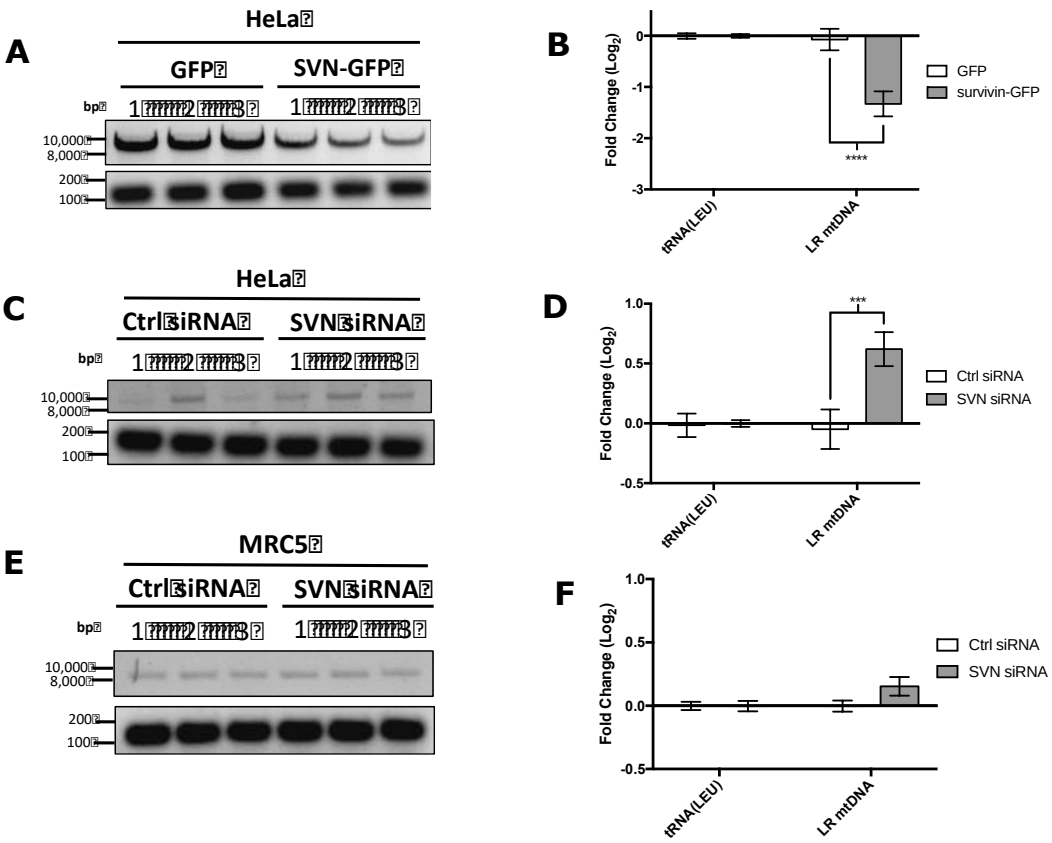

Figure 7
Townley and Wheatley, 2020

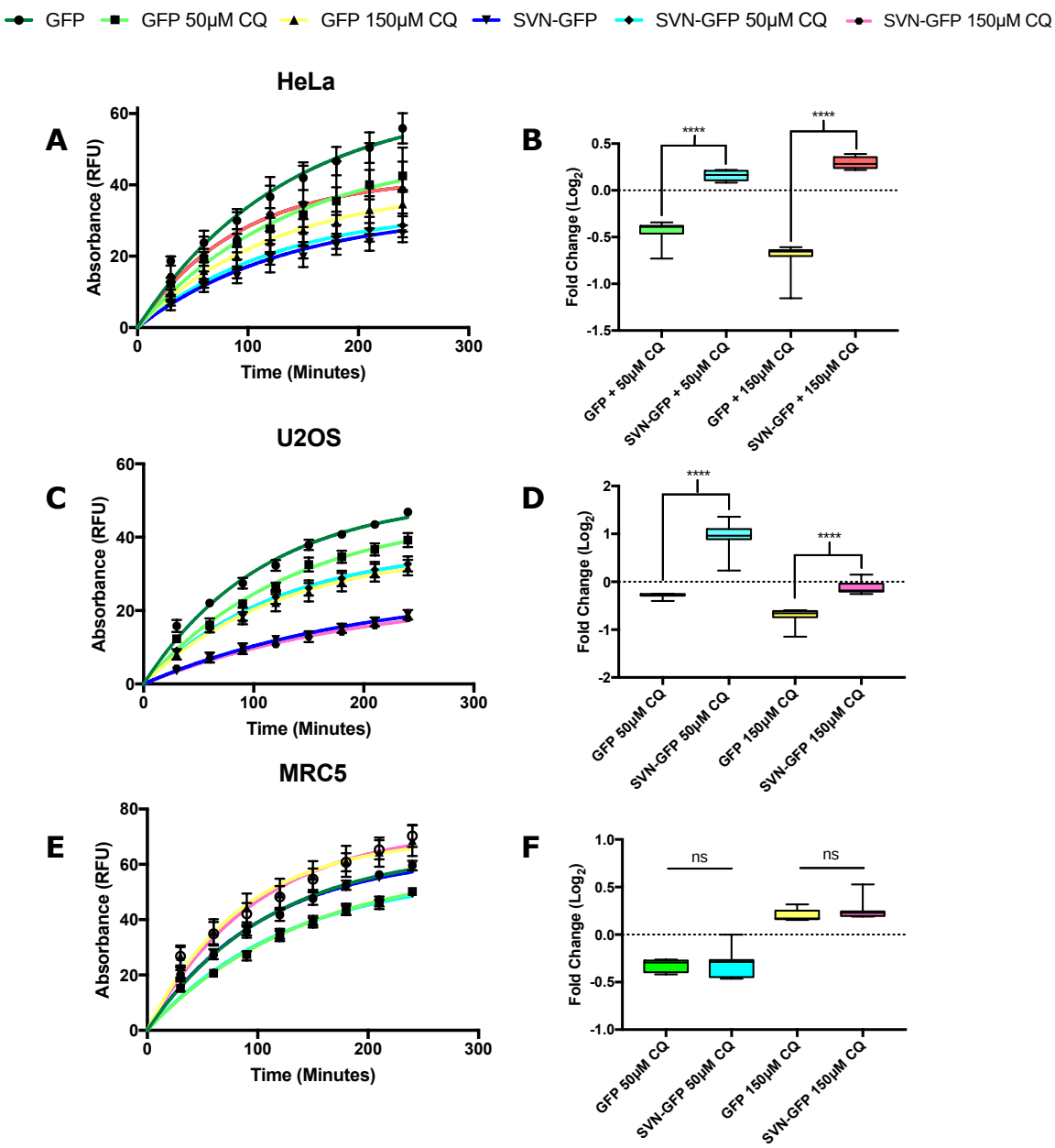

Figure 8
Townley and Wheatley, 2020